

Structure and Equation of State of Neutron Stars: General Overview

OUTER LAYER
1 meter thick
solid or liquid

CORE
10-15 kilometer deep
liquid

Nicolas Chamel

Institute of Astronomy and Astrophysics
Université Libre de Bruxelles, Belgium



ULB

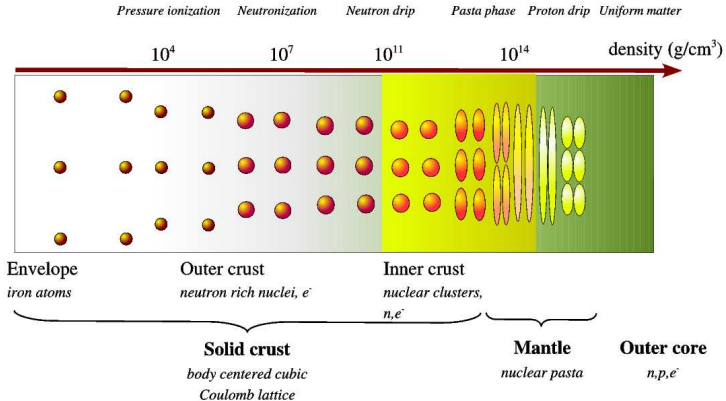


CRUST
1 kilometer thick
solid

CEA, Saclay, 8 December 2017

NEUTRON STAR

Neutron star interiors: a variety of phases

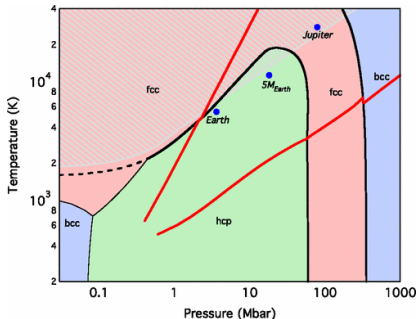


Chamel & Haensel, *Living Reviews in Relativity* 11 (2008), 10

The inner core of neutron stars might contain other particles such as hyperons and deconfined quarks under various phases.

Structure of the outermost layers

The surface of a neutron star is made of **iron, the end product of stellar nucleosynthesis** (identification of broad Fe K emission lines from accretion disk around neutron stars in LMXB).



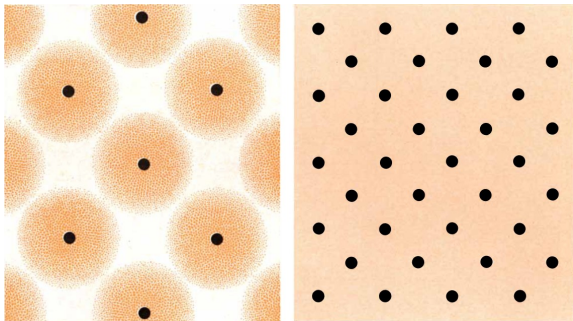
Compressed iron can be studied with **nuclear explosions and laser-driven shock-wave experiments**... but at pressures corresponding to about 0.1 mm below the surface of a neutron star with a mass $\mathcal{M} = 1.4\mathcal{M}_{\odot}$ and a radius $R = 12$ km !

Stixrude, Phys. Rev. Lett. 108, 055505 (2012)

Ab initio calculations predict various **structural phase transitions**.

Crystal Coulomb plasma

At a density $\rho_{\text{eip}} \approx 2 \times 10^4 \text{ g cm}^{-3}$ (about 22 cm below the surface), the interatomic spacing becomes comparable with the atomic radius.



Ruderman, Scientific American 224, 24 (1971)

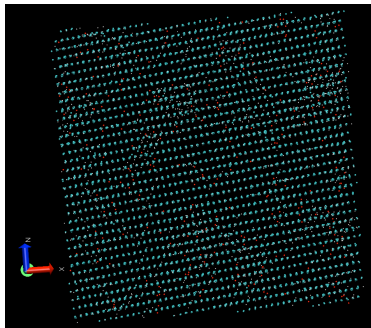
- At densities $\rho \gg \rho_{\text{eip}}$, atoms are crushed into a **dense plasma of nuclei and free electrons**.
- Nuclei form a body-centered cubic (bcc) lattice crystal.

Accreted crust

The composition of the surface layers may be changed by

- the **fallback** of material from the supernova explosion,
- the **accretion** of matter from a stellar companion (X-ray bursts).

The equilibrium structure of multicomponent plasmas is uncertain



Classical molecular dynamics simulations predict the formation of a **regular crystal or polycrystals**.

However, the system may have not fully relaxed to its true equilibrium.

Search of the equilibrium structure using genetic algorithms but restricted to O-Fe-S and Fe-As-Se.

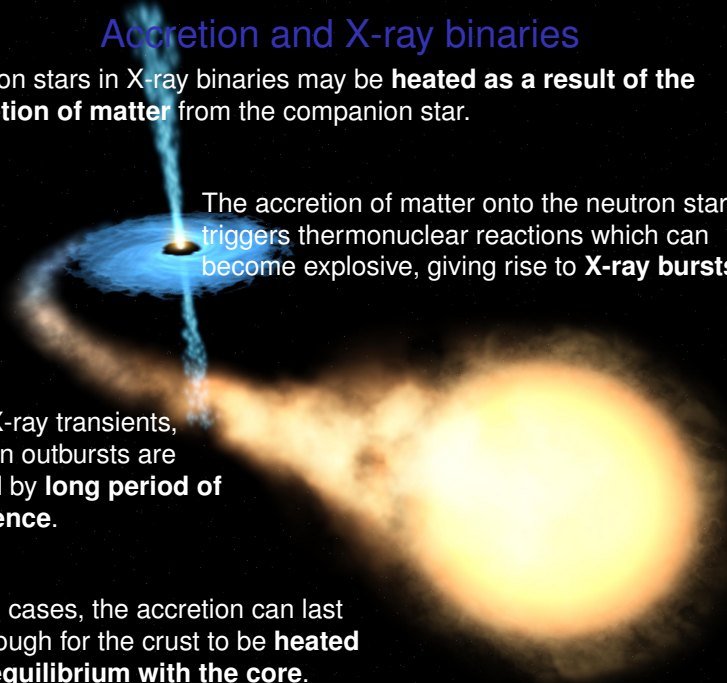
Engstrom et al., ApJ.818, 183 (2016)

Horowitz, Berry, Phys.Rev.C79, 065803 (2009)

Horowitz et al., Phys.Rev.E79, 2 (2009)

Accretion and X-ray binaries

Neutron stars in X-ray binaries may be **heated as a result of the accretion of matter** from the companion star.



The accretion of matter onto the neutron star triggers thermonuclear reactions which can become explosive, giving rise to **X-ray bursts**.

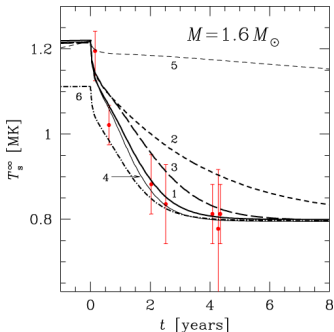
In soft X-ray transients, accretion outbursts are followed by **long period of quiescence**.

In some cases, the accretion can last long enough for the crust to be **heated out of equilibrium with the core**.

Thermal relaxation of soft x-ray transients

The thermal relaxation during the quiescent state has been monitored for a few accreting neutron stars.

Waterhouse et al., MNRAS 456, 4001 (2016)



Example: KS 1731–260

Curves 1,3,4 : crystalline crust with neutron superfluidity

Curve 2 : crystalline crust without neutron superfluidity

Curve 4 : perfect crystal with weak neutron superfluidity

Curve 5 : amorphous crust with neutron superfluidity

Shternin et al., MNRAS, L43382(2007)

Brown&Cumming, ApJ698;1020 (2009)

Page&Reddy, Neutron Star Crust, eds Bertulani&Piekarewicz (Nova Science Publishers, New York, 2012) p. 281.

Observations indicate that accreted crusts are not amorphous solids.



Highly-magnetised crust

At the surface of neutron stars $B \lesssim 2 \times 10^{15}$ G.

The electron motion perpendicular to \mathbf{B} is quantised into **Landau orbitals** with a characteristic scale $a_m = a_0 \sqrt{B_{\text{at}}/B}$, where a_0 is the Bohr radius

For $B \gg B_{\text{at}} = m_e^2 e^3 c / \hbar^3 \simeq 2.35 \times 10^9$ G, atoms are expected to adopt a very elongated shape along \mathbf{B} and to form **linear chains**
Ruderman, PRL27, 1306 (1971); Medin&Lai, Phys.Rev. A74, 062508 (2006)

The attractive interaction between these chains could lead to a transition into a **condensed phase** with a surface density

$$\rho_s \sim 560AZ^{-3/5}(B/10^{12} \text{ G})^{6/5} \text{ g cm}^{-3}$$

In deeper regions of the crust,

$$\rho \approx \rho_s \left(1 + \sqrt{\frac{P}{P_0}} \right), \quad P_0 \simeq 1.45 \times 10^{20} (B/10^{12} \text{ G})^{7/5} \left(\frac{Z}{A} \right)^2 \text{ dyn cm}^{-2}$$

Lai, Rev.Mod.Phys.73, 629 (2001); Chamel et al., Phys.Rev.C86, 055804 (2012)

The intriguing case of RX J1856.5-3754

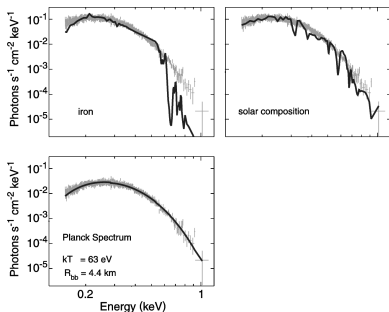
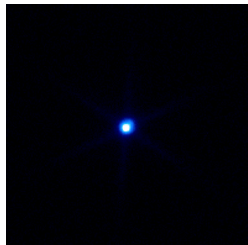


Fig. 3: The Chandra LETG X-ray spectrum of RX J1856 fitted with (non-magnetic) photospheric models assuming pure iron and solar composition. The best fit is obtained with a Planck spectrum (Burwitz et al. 2003).



X-ray observations with Chandra

Turolla et al., ApJ 603, 265 (2004)

van Adelsberg et al., ApJ 628, 902 (2005)

Trümper (2005), astro-ph/0502457

Recent review: *Potekhin et al., Space Sci. Rev. 191, 171 (2015)*

The thermal X-ray emission is best fitted by a **black body** spectrum: evidence for a condensed surface? The presence of high **B** has found additional support from recent optical polarimetry measurements.

Mignani et al., MNRAS 465, 492 (2017)

Description of the outer crust of a neutron star

Main assumptions:

- **cold “catalysed” matter** (full thermodynamic equilibrium)
Harrison, Wakano and Wheeler, Onzième Conseil de Physique Solvay (Stoops, Brussels, Belgium, 1958) pp 124-146

- the crust is stratified into **pure layers** made of nuclei A_ZX
- electrons are uniformly distributed and are highly degenerate
 $T < T_F \approx 5.93 \times 10^9 (\gamma_r - 1) \text{ K}$

$$\gamma_r \equiv \sqrt{1 + x_r^2}, \quad x_r \equiv \frac{\rho_F}{m_e c} \approx 1.00884 \left(\frac{\rho_6 Z}{A} \right)^{1/3}$$

- nuclei are arranged on a **perfect body-centered cubic lattice**
 $T < T_m \approx 1.3 \times 10^5 Z^2 \left(\frac{\rho_6}{A} \right)^{1/3} \text{ K} \quad \rho_6 \equiv \rho / 10^6 \text{ g cm}^{-3}$

Tondeur, A&A 14, 451 (1971)

Baym, Pethick, Sutherland, ApJ 170, 299 (1971).

Neutron-star crust and nuclear masses

The ground-state composition of the outer crust is completely determined by **nuclear masses** $M'(A, Z)$.

In the limit of ultrarelativistic electron Fermi gas:

$$P_{1 \rightarrow 2} \approx \frac{(\mu_e^{1 \rightarrow 2})^4}{12\pi^2(\hbar c)^3}, \quad \bar{n}_1^{\max} \approx \frac{A_1}{Z_1} \frac{(\mu_e^{1 \rightarrow 2})^3}{3\pi^2(\hbar c)^3}, \quad \bar{n}_2^{\min} \approx \frac{A_2}{Z_2} \frac{Z_1}{A_1} \bar{n}_1^{\max}$$
$$\mu_e^{1 \rightarrow 2} \equiv \left[\frac{M'(A_2, Z_2)c^2}{A_2} - \frac{M'(A_1, Z_1)c^2}{A_1} \right] \left(\frac{Z_1}{A_1} - \frac{Z_2}{A_2} \right)^{-1} + m_e c^2$$

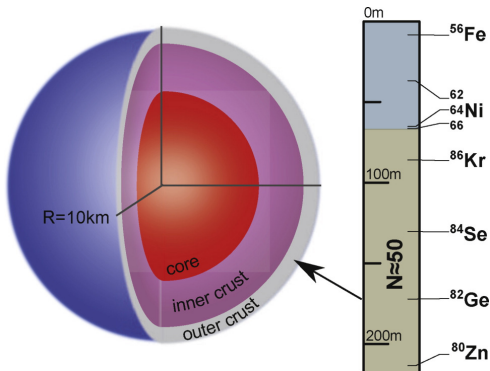
Since $\bar{n}_2^{\min} > \bar{n}_1^{\max}$ in hydrostatic equilibrium, matter becomes more **neutron rich** ($Z_2/A_2 < Z_1/A_1$) with increasing depth.

Essentially exact **analytical expressions** valid for any degree of relativity of the electron gas and including electrostatic correction:

Chamel&Fantina, Phys. Rev. C94, 065802(2016)

Experimental “determination” of the outer crust

The composition of the crust is completely determined by experimental nuclear masses down to about 200m for a $1.4M_{\odot}$ neutron star with a 10 km radius



The physics governing the structure of atomic nuclei (magicity) leaves its imprint on the composition.

Due to β equilibrium and electric charge neutrality, Z is more tightly constrained than N : only a few layers with $Z = 28$.

Plumbing neutron stars to new depths

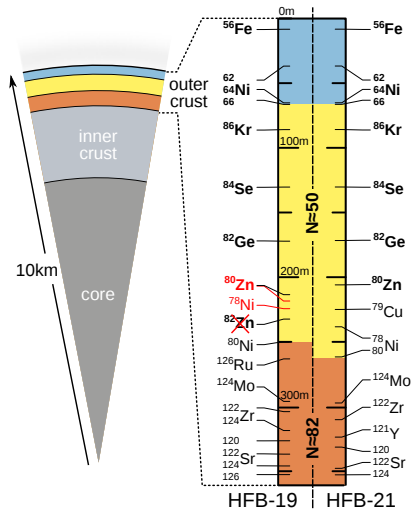
Precision measurements of the mass of short-lived zinc nuclides by the ISOLTRAP collaboration at CERN's ISOLDE radioactive-beam facility in 2013 allowed to "drill" deeper into the crust.

Wolf et al., PRL 110, 041101 (2013).

The composition is very sensitive to small corrections such as electron screening.

Chamel & Fantina, Phys. Rev. D 93, 063001 (2016)

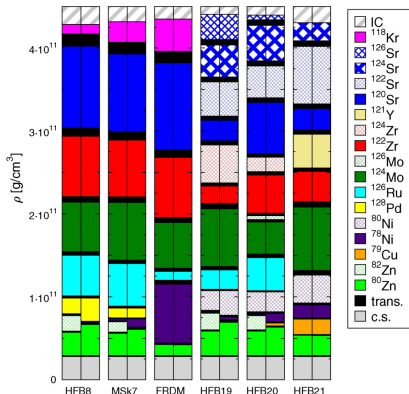
Errors on nuclear masses of a few keV can also change the composition!



Theoretical predictions of the outer crust

Deeper in the crust, recourse must be made to nuclear mass models:

- semi-empirical formulas (e.g. Bethe & Weizsäcker) – $\sigma \sim 3$ MeV
- mic-mac models (e.g. Duflo & Zücker, FRDM) – $\sigma \sim 0.3-0.5$ MeV
- microscopic models (e.g. HFB) – $\sigma \sim 0.5$ MeV



Some recent calculations:

Pearson et al., Phys.Rev.C83,065810(2011)

Kreim et al., Int.J.M.Spec.349-350,63(2013)

Sharma et al., A&A 584, A103 (2015)

Utama et al., Phys.Rev.C93,014311(2016).

Note: odd nuclei ^{79}Cu , ^{121}Y

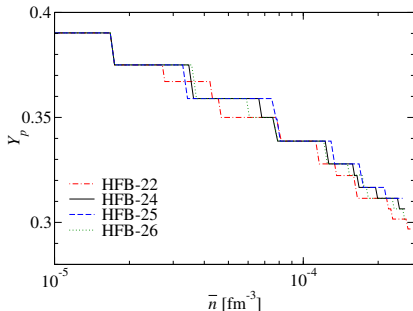
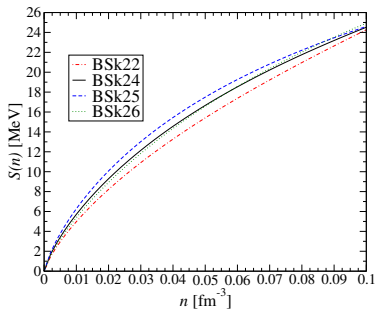
Only microscopic models can also be used to describe the inner crust and the core of a neutron star.

Role of the symmetry energy

The composition of the outer crust is influenced by the density dependence of the symmetry energy below saturation density.

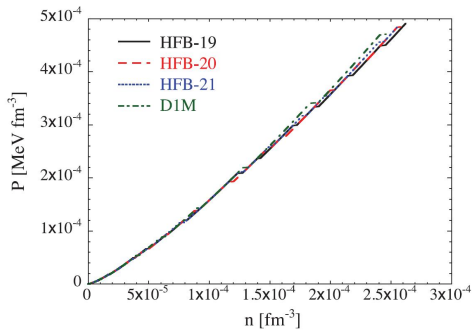
The proton fraction varies roughly as

$$Y_p = \frac{Z}{A} \sim \frac{1}{2} - \frac{(12\pi^2(\hbar c)^3 P)^{1/4}}{8S}$$

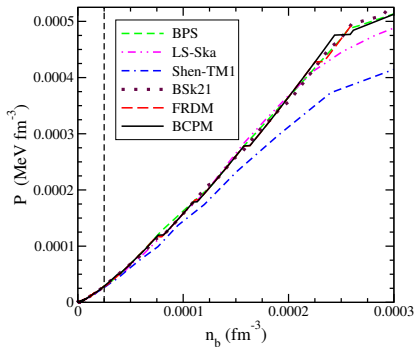


Equation of state of the outer crust

The pressure, dominated by that of the electron Fermi gas, is almost independent of the composition.



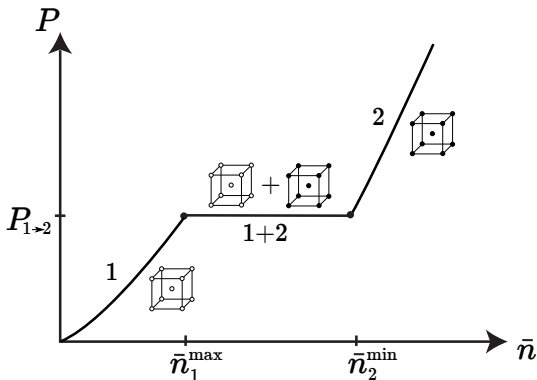
Pearson et al., Phys.Rev.C83,065810(2011)



Sharma et al., A&A 584, A103 (2015)

Stratification and equation of state

Transitions between adjacent crustal layers are accompanied by **density discontinuities**.



Mixed solid phases cannot exist in a neutron star crust because P has to increase strictly monotonically with \bar{n} (hydrostatic equilibrium).

Compounds in neutron-star crusts?

Multinary ionic compounds made of nuclei with charges $\{Z_i\}$ might exist in the crust of a neutron star.

Dyson, Ann. Phys.63, 1 (1971); Witten, ApJ 188, 615 (1974)

Necessary conditions:

- **stability against weak and strong nuclear processes.**
Jog&Smith, ApJ 253, 839(1982).
- **stability against the separation into pure (bcc) phases:**

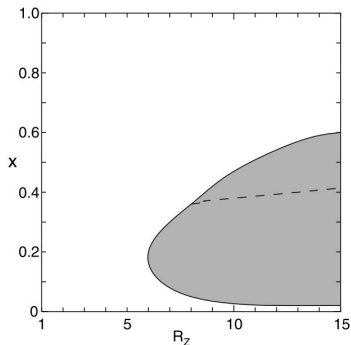
$$\mathcal{R}(\{Z_i/Z_j\}) \equiv \frac{C}{C_{\text{bcc}}} f(\{Z_i\}) \frac{\bar{Z}}{Z^{5/3}} > 1$$

where $f(\{Z_i\})$ is the dimensionless lattice structure function of the compound and C the corresponding structure constant.

Chamel & Fantina, Phys. Rev. C94, 065802 (2016).

Ordered vs disordered compounds

Amorphous solids in accreted crusts are disfavored by observations of SXT. Nonaccreted crusts are unlikely to be less ordered.

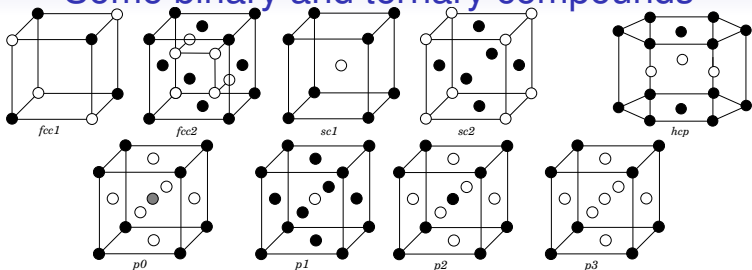


Stability of disordered binary Coulomb compounds with charge ratios $R_Z = Z_2/Z_1$ and composition $x = N_2/N$ against phase separation (shaded area)

Igarashi, Nakao, and Iyetomi, *Contrib. Plasma Phys.* 41, 319 (2001).

For the charge ratios expected in nonaccreted neutron-star crusts, disordered compounds are unstable.

Some binary and ternary compounds



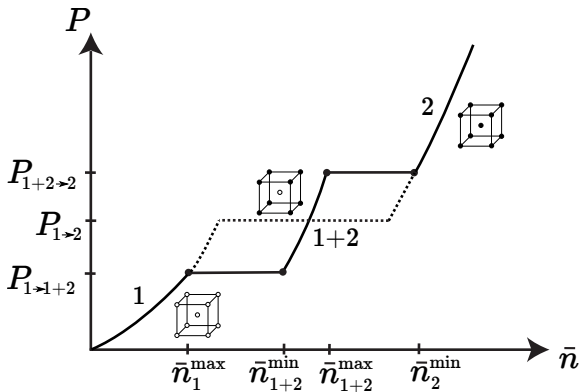
Terrestrial examples:

- *fcc1*: rocksalt (NaCl), oxides (MgO), carbonitrides (TiN)
- *fcc2*: fluorite (CaF₂)
- *sc1*: cesium chloride (CsCl), β -brass (CuZn)
- *sc2*: auricupride (AuCu₃)
- *hcp*: tungsten carbide (WC)
- *p0*: perovskite (BaTiO₃)

Stellar vs terrestrial compounds: (i) they are made of nuclei; (ii) electrons form an essentially uniform relativistic Fermi gas.

Substitutional compounds in neutron-star crusts

Compounds with CsCl structure are present at interfaces if $Z_1 \neq Z_2$.



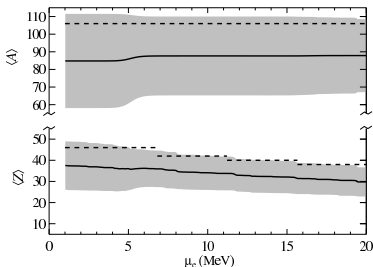
But they only exist over an extremely small range of pressures.

Chamel&Fantina, *Phys. Rev. C*94, 065802 (2016).

Composition of accreted neutron star crusts

Accreted crusts are not in full thermodynamic equilibrium.

- The composition depends on the nuclear processes during X-ray (super)bursts.
- Ashes may be further more slowly processed (electron captures, pycnonuclear reactions) as they sink deeper inside the star.



— *Gupta et al. (2007)*

- - - *Haensel&Zdunik(2003)*

Different approaches:

- one-component liquid drop models
Haensel& Zdunik, A&A404, L33 (2003)
Haensel&Zdunik, A&A480, 459 (2008)
- multicomponent liquid drop models
Steiner, Phys.Rev.C85, 055804 (2012)
- reaction networks
Gupta et al., ApJ662, 1188(2007)

Impact of a high magnetic field on the crust?

In a high magnetic field \vec{B} (along let's say the z-axis), the **electron motion perpendicular to the field is quantised**:



$$e_\nu = \sqrt{c^2 p_z^2 + m_e^2 c^4 (1 + 2\nu B_\star)}$$

where $\nu = 0, 1, 2, \dots$ and $B_\star = B/B_c$

$$\text{with } B_c = \frac{m_e^2 c^3}{\hbar e} \simeq 4.4 \times 10^{13} \text{ G.}$$

Rabi, Z.Phys.49, 507 (1928).

Maximum number of occupied Landau levels for HFB-21:

B_\star	1500	1000	500	100	50	10	1
ν_{\max}	1	2	3	14	28	137	1365

Only $\nu = 0$ is filled for $\rho < 2.07 \times 10^6 (A/Z) B_\star^{3/2} \text{ g cm}^{-3}$.

Electron quantisation impacts the properties of the outer crust.

Chamel et al., Phys.Rev.C86, 055804(2012)

Nandi&Bandyopadhyay, J.Phys.Conf.Ser.420, 012144 (2013)

Basilico et al., Phys.Rev. C92, 035802 (2015)

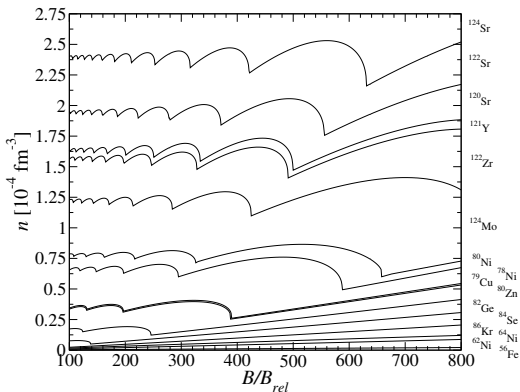
Composition of the outer crust of a magnetar

The composition depends on B , but not the structure (bcc).

Kozhberov, Astrophys. Space Sci.361, 256 (2016)

Equilibrium nuclides for HFB-24 and $B_* \equiv B/(4.4 \times 10^{13} \text{ G})$:

Nuclide	B_*
$^{58}\text{Fe}(-)$	9
$^{66}\text{Ni}(-)$	67
$^{88}\text{Sr}(+)$	859
$^{126}\text{Ru}(+)$	1031
$^{80}\text{Ni}(-)$	1075
$^{128}\text{Pd}(+)$	1445
$^{78}\text{Ni}(-)$	1610
$^{79}\text{Cu}(-)$	1617
$^{64}\text{Ni}(-)$	1668
$^{130}\text{Cd}(+)$	1697
$^{132}\text{Sn}(+)$	1989



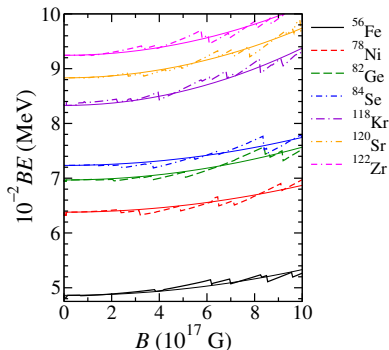
Chamel et al., Progress in Theoretical Chemistry & Physics (Springer, 2017), pp 181-191.

Composition of the outer crust of a magnetar

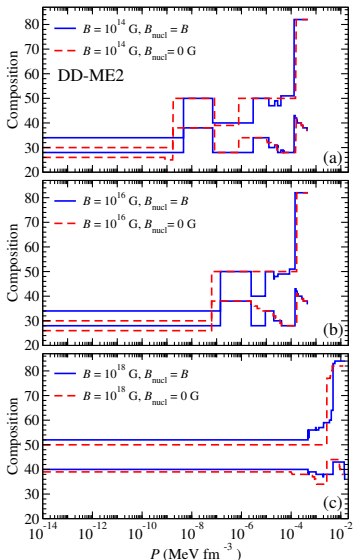
High enough magnetic fields can change the structure of nuclei.

Peña Arteaga et al., PRC84,045806(2011)

Stein et al., PRC94,035802(2016)



Right: crust composition obtained for a *reduced* set of nuclei.

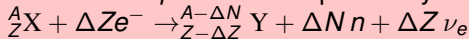


Basilico et al., PRC92, 035802 (2015)

Neutron-drip transition: general considerations

With increasing pressure, nuclei become progressively more neutron rich until neutrons start to drip out.

Nuclei are actually stable against neutron emission but are unstable against *electron captures* accompanied by neutron emission



- nonaccreting (catalysed) neutron stars**

All kinds of reactions are allowed: the ground state is reached for $\Delta Z = Z$ and $\Delta N = A$

	outer crust	drip line	ρ_{drip} (g cm ⁻³)	P_{drip} (dyn cm ⁻²)
HFB-19	¹²⁶ Sr (0.73)	¹²¹ Sr (-0.62)	4.40×10^{11}	7.91×10^{29}
HFB-20	¹²⁶ Sr (0.48)	¹²¹ Sr (-0.71)	4.39×10^{11}	7.89×10^{29}
HFB-21	¹²⁴ Sr (0.83)	¹²¹ Sr (-0.33)	4.30×10^{11}	7.84×10^{29}

- accreting neutron stars**

Multiple electron captures are very unlikely: $\Delta Z = 1$ ($\Delta N \geq 1$)

	ρ_{drip} (g cm ⁻³)	P_{drip} (dyn cm ⁻²)
HFB-21	$2.83 - 5.84 \times 10^{11}$	$4.79 - 12.3 \times 10^{29}$

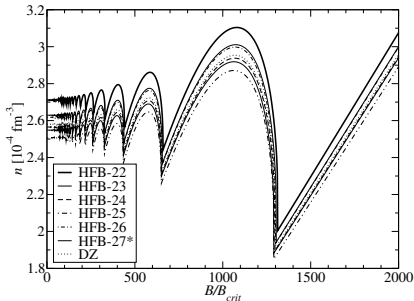
ρ_{drip} and P_{drip} can be expressed by analytical formulas.

Chamel et al., *Phys.Rev.C*91,055803(2015).

Neutron-drip transition in magnetars

The neutron drip density exhibits typical **quantum oscillations**.

Example using HFB-24:



Universal oscillations:

$$\frac{n_{\text{drip}}^{\text{min}}}{n_{\text{drip}}(B_{\star} = 0)} \approx \frac{3}{4}$$

$$\frac{n_{\text{drip}}^{\text{max}}}{n_{\text{drip}}(B_{\star} = 0)} \approx \frac{35 + 13\sqrt{13}}{72}$$

In the strongly quantising regime,

$$n_{\text{drip}} \approx \frac{A}{Z} \frac{\mu_e^{\text{drip}}}{m_e c^2} \frac{B_{\star}}{2\pi^2 \lambda_e^3} \left[1 - \frac{4}{3} C_{\alpha} Z^{2/3} \left(\frac{B_{\star}}{2\pi^2} \right)^{1/3} \left(\frac{m_e c^2}{\mu_e^{\text{drip}}} \right)^{2/3} \right]$$

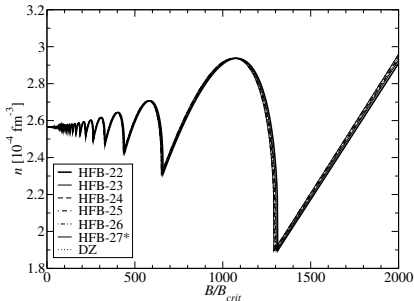
Chamel et al., *Phys.Rev.C*91, 065801(2015).

Chamel et al., *J.Phys.:Conf.Ser.*724, 012034 (2016).

Neutron-drip transition in magnetars

The neutron drip density exhibits typical **quantum oscillations**.

Example using HFB-24:



Universal oscillations:

$$\frac{n_{\text{drip}}^{\text{min}}}{n_{\text{drip}}(B_{\star} = 0)} \approx \frac{3}{4}$$

$$\frac{n_{\text{drip}}^{\text{max}}}{n_{\text{drip}}(B_{\star} = 0)} \approx \frac{35 + 13\sqrt{13}}{72}$$

In the strongly quantising regime,

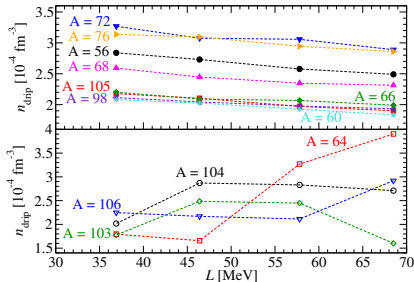
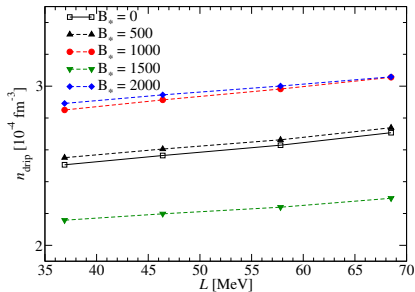
$$n_{\text{drip}} \approx \frac{A}{Z} \frac{\mu_e^{\text{drip}}}{m_e c^2} \frac{B_{\star}}{2\pi^2 \lambda_e^3} \left[1 - \frac{4}{3} C_{\alpha} Z^{2/3} \left(\frac{B_{\star}}{2\pi^2} \right)^{1/3} \left(\frac{m_e c^2}{\mu_e^{\text{drip}}} \right)^{2/3} \right]$$

Chamel et al., *Phys.Rev.C*91, 065801(2015).

Chamel et al., *J.Phys.:Conf.Ser.*724, 012034 (2016).

Neutron-drip transition: role of the symmetry energy

The lack of knowledge of the symmetry energy translates into uncertainties in the neutron-drip density:

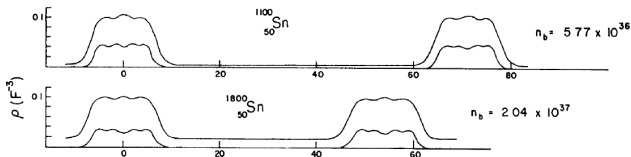


Fantina et al., Phys.Rev.C93,015801(2016).

In accreted crusts, the neutron-drip transition may be more sensitive to nuclear-structure effects than the symmetry energy.

Description of the inner crust of a neutron star

The conditions prevailing in the inner crust of a neutron star cannot be reproduced in terrestrial laboratories:



Negele & Vautherin, Nucl. Phys. A207, 298 (1973)

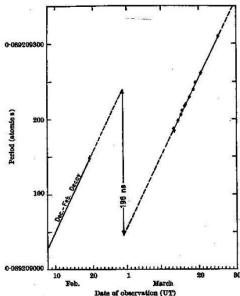
- The **neutron-saturated clusters** owe their existence to the presence of a highly degenerate surrounding neutron liquid.
- Unbound neutrons are expected to be **superfluid** at $T \leq T_c$ by forming Cooper pairs analogously to electrons in conventional superconductors.

State-of-the-art calculations rely on the self-consistent **nuclear energy density functional theory**.

Duguet, Lect. Notes Phys. 879 (Springer-Verlag Berlin Heidelberg, 2014), pp 293-350.

Pulsar sudden spin-ups and superfluidity

Neutron-star superfluidity was predicted by Migdal, and first studied by Ginzburg & Kirzhnits **before the discovery of pulsars**.



Some pulsars suddenly spin up ($\lesssim 1$ minute).

493 glitches have been detected in 168 pulsars.

<http://www.jb.man.ac.uk/pulsar/glitches.html>

Pulsar glitches provide the strongest evidence of nuclear superfluidity in neutron stars

- long relaxation times (months-years)
- glitches observed in He II.

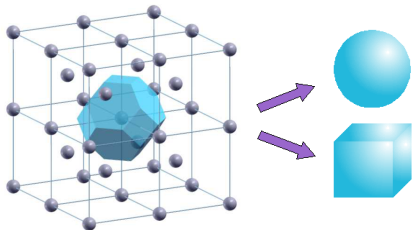
Superfluidity may leave its imprint on other phenomena, e.g. thermal relaxation of SXT, QPOs in SGRs.

Some recent review:

Chamel, J. Astrophys. Astr.38, 43 (2017) - special issue in honor of Prof. Srinivasan

Implementations of the HFB equations

Assuming the crust is a **perfect (bcc) crystal**, the HFB equations need to be solved only inside one Wigner-Seitz cell of the lattice.



- **Wigner-Seitz approximation**

Pastore et al., J.Phys.G44, 094003(2017)

Grill et al., PRC84, 065801(2011)

Baldo et al., PRC76, 025803(2007)

- **cubic box with periodic boundary conditions**

Gögelein&Müther, PRC76, 024312 (2007)

Magierski&Heenen, PRC65,045804(2002)

The crustal composition was found to depend on nuclear pairing

But such calculations are limited by **spurious neutron shell effects**.

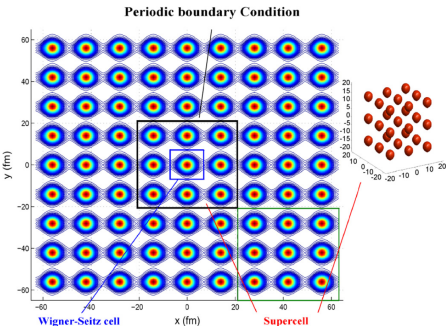
Fattoyev et al., PRC95,055804(2017); Newton&Stone, PRC79,055801 (2009)

Margueron et al., in Exotic States of Nuclear Matter, Eds Lombardo, Baldo, Burgio, Schulze (World Scientific Publishing, 2008), p.362

Chamel et al., PRC75,055806(2007)

Implementations of the HFB equations

Going beyond:



Sébille et al., Nucl.Phys.A822,51(2009)

- **"Supercell"**

Sébille et al., PRC 84, 055801 (2011)

The results can be biased by the choice of the "supercell"

Giménez Molinelli&Dorso,

Nucl.Phys.A933,306 (2015)

- **Bloch boundary conditions**

Schuetrumpf&Nazarewicz, PRC92,045806(2015)

Chamel, PRC85,035801(2012)

Requires the a priori knowledge of the crystal structure

Both approaches are computationally extremely costly: no systematic calculations of neutron-star crust matter so far

Fast numerical implementation of HFB equations

We use the **Extended Thomas-Fermi+Strutinsky Integral (ETFSI)** approach with the *same* functional as in the outer crust:

- **semiclassical expansion in powers of \hbar^2** : the energy becomes a functional of $n_q(\mathbf{r})$ and their gradients only.
- **proton shell effects** are added perturbatively (neutron shell effects are much smaller and therefore neglected).

In order to further speed-up the calculations, clusters are supposed to be spherical (no pastas) and $n_q(\mathbf{r})$ are parametrized.

Pearson,Chamel,Pastore,Goriely,Phys.Rev.C91, 018801 (2015).

Pearson,Chamel,Goriely,Ducoin,Phys.Rev.C85,065803(2012).

Onsi,Dutta,Chatri,Goriely,Chamel,Pearson, Phys.Rev.C77,065805 (2008).

Advantages of the ETFSI method:

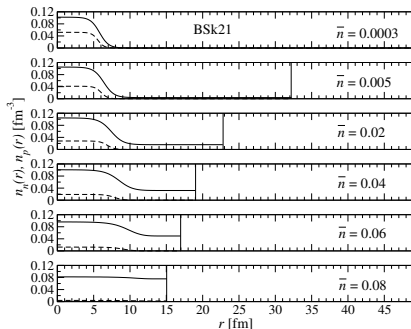
- very fast approximation to the full HFB equations
- avoids the pitfalls related to boundary conditions

Structure of nonaccreting neutron star crusts

With increasing density, the clusters keep essentially the same size but become more and more dilute.

Crust-core transition properties

	\bar{n}_{cc} (fm^{-3})	P_{cc} (MeV fm^{-3})
BSk29	0.0814	0.263
BSk28	0.0808	0.266
BSk27*	0.0919	0.439
BSk26	0.0849	0.363
BSk25	0.0856	0.211
BSk24	0.0808	0.268
BSk22	0.0716	0.291
BSk21	0.0809	0.268
BSk20	0.0854	0.365
BSk19	0.0885	0.428

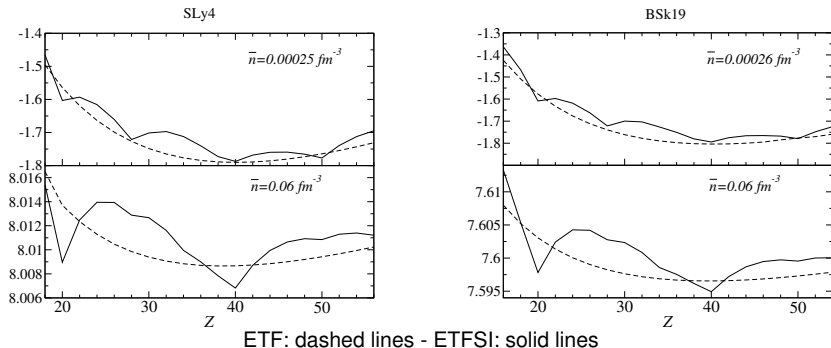


Chamel et al., *Acta Phys.Pol.*46,349(2015); Pearson et al., *PRC*91,018801(2015)
Pearson et al., *Phys.Rev.C*85,065803(2012)

The crust-core transition is found to be very smooth.

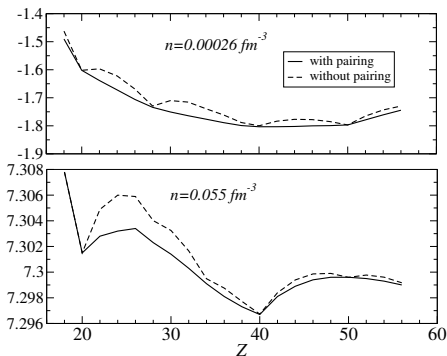
Role of proton shell effects on the composition of the inner crust of a neutron star

- The ordinary nuclear shell structure is changed: disappearance of $Z = 28, 82$, appearance of 40, 58, 92 (quenched spin-orbit).
- The energy differences between different configurations become very small as the density increases!



Role of proton pairing on the composition of the inner crust of a neutron star

Proton shell effects are reduced by pairing.



Example with BSk21.

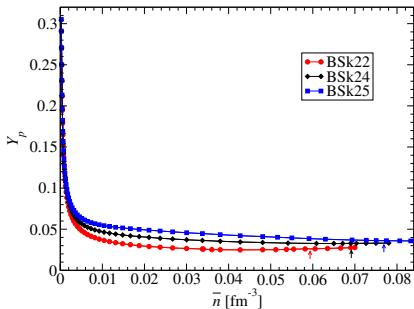
At low densities, $Z = 42$ is energetically favored over $Z = 40$, but by less than 5×10^{-4} MeV per nucleon.

A large range of values of Z could be present in the deeper crust.

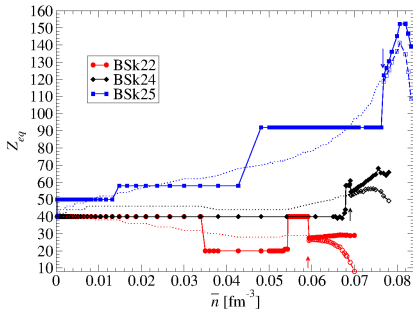
Pearson et al., *Phys.Rev.C91*, 018801 (2015).

Role of shell effects and symmetry energy

The composition of the inner crust is still found to be strongly influenced by proton shell effects and by the symmetry energy.



Pearson et al., in prep.



ETF: dashed lines - ETFSI: solid lines

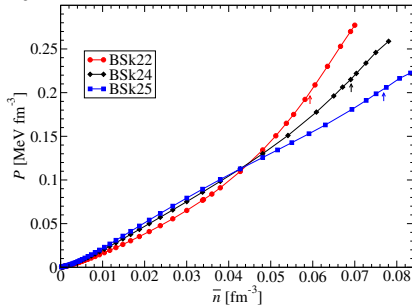
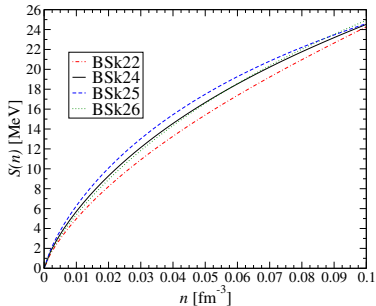
At high enough densities, clusters are found to coexist with free neutrons and **free protons**.

Equation of state

The pressure in the inner crust is related to the slope L of the symmetry energy: the higher the slope, the stiffer the equation of state.

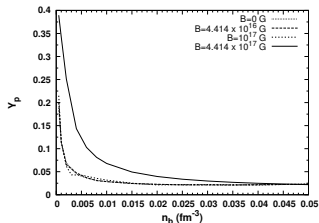
The pressure is mainly determined by the neutron gas

$$P \sim \frac{L}{3} \frac{n_n^2}{n_0}$$



Pearson et al., in prep.

Role of a high magnetic field on the inner crust of a neutron star

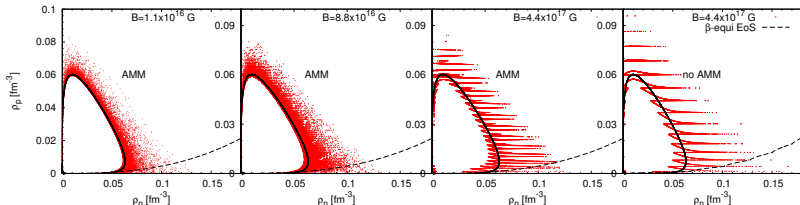


Rabi quantisation of electron motion was studied in the TF approximation

- the neutron liquid is more dilute
- clusters are larger and closer

Nandi et al., ApJ736, 156 (2011)

Accounting as well for quantisation of nucleon motion, the crust is expected to be **less neutron rich and highly heterogeneous**.

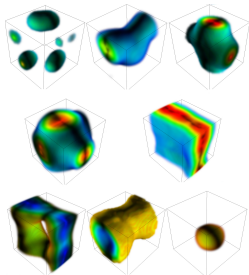


Chen, PRC95,035807(2017); Fang et al., PRC95,045802(2017)

Nuclear "pastas"

Nuclear "pastas" were first predicted based on liquid drop models.

Ravenhall et al., PRL50, 2066 (1983); Hashimoto et al., PTP71, 320 (1984)



Schuetrumpf et al., PRC87, 055805 (2013)

Nuclear "pastas" have been studied using liquid-drop models, semiclassical methods, and nuclear EDF theory.

Chamel&Haensel, Liv. Rev. Relativ. 11 (2008), 10
Watanabe&Maruyama, in Neutron Star Crust, Eds
Bertulani&Piekarowicz (Nova Science Publishers,
2012), p. 23

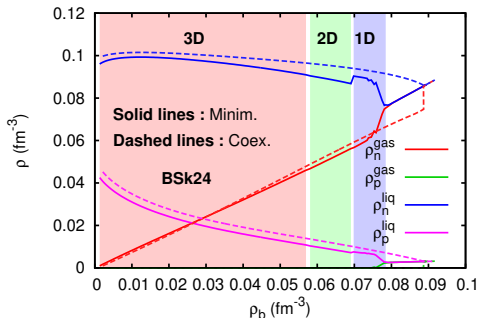
In all these approaches, a few specific nuclear shapes are generally considered, or some symmetries are assumed.

Some models do not predict the occurrence of pastas.

Nuclear "pastas"

If they exist, pastas follow the sequence: gnocchi/polpette (spheres), spaghetti (cylinders), lasagna (slabs), bucatini/penne/maccheroni (cylindrical bubbles), Swiss cheese/scaciatta (bubbles).

Extended Thomas-Fermi (2nd order) with BSk24
(no shell corrections, different parametrization of $n_q(\mathbf{r})$):



Nuclear "pasta" formation

The formation of nuclear pastas has been explored using large scale molecular dynamics in a box with periodic boundary conditions.

Dorso et al., in Neutron Star Crust, Eds Bertulani&Piekarewicz (Nova Science Publishers, New York, 2012), pp. 151-169.

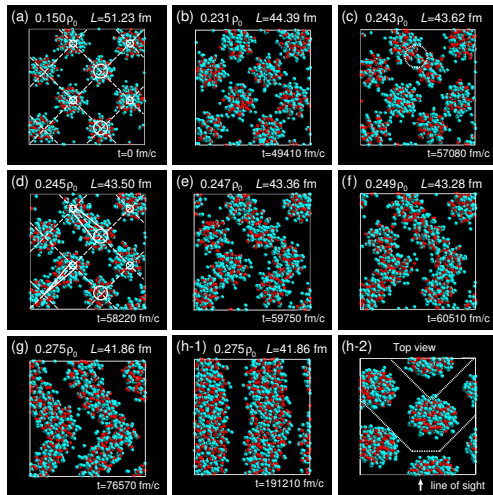
- **classical molecular dynamics** ($N \sim 10^3 - 10^5$)
pointlike particles interacting through a two-body potential
Berry et al., PRC94,055801(2016); Dorso et al., PRC86,055805(2012)
- **quantum molecular dynamics** ($N \sim 10^3$)
Gaussian wave packets moving (classically) in a mean field.
Phenomenological antisymmetrisation (Pauli potential).
Maruyama et al., Prog.Theor.Exp.Phys. 2012,01A201(2012)
- **fermionic molecular dynamics** (very costly, scale as N^4 vs N^2)
Slater determinants.
Vantournhout et al.,Prog.Part.Nucl.Phys.66,271(2011); Vantournhout&Feldmeier, J.Phys.Conf.Ser.342,012011(2012)

Results could be influenced by the geometry of the box and the treatment of Coulomb interactions.

Giménez Molinelli&Dorso,NPA933,306 (2015); Alcain et al., PRC89,055801(2014)

Nuclear "pasta" formation

As clusters get closer with increasing density, they eventually fuse and connect into herringbone structures turning into "spaghettis".



Unified equations of state of neutron stars

The same functionals used in the crust can be also used in the core (n, p, e^-, μ^-) thus providing a **unified and thermodynamically consistent description of neutron stars**.

- **Tables** of equations of state for BSk19, BSk20, BSk21:

<http://vizier.cfa.harvard.edu/viz-bin/VizieR?-source=J/A+A/559/A128>
Fantina, Chamel, Pearson, Goriely, A&A 559, A128 (2013)

- **Analytical representations** (fortran subroutines):

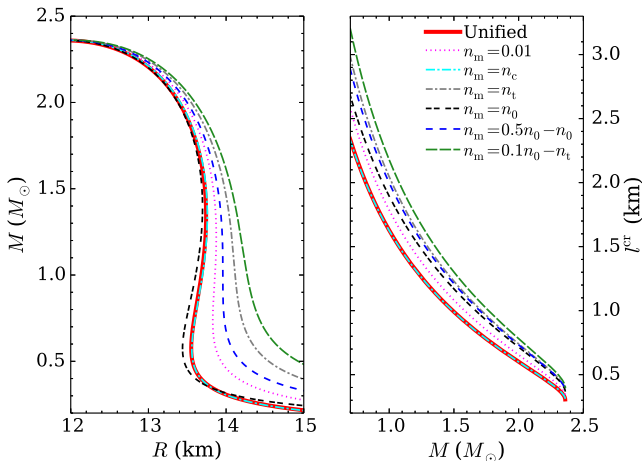
<http://www.ioffe.ru/astro/NSG/BSk/>
Potekhin, Fantina, Chamel, Pearson, Goriely, A&A 560, A48 (2013)

Equations of state for BSk22-26 will appear soon.

Pearson et al., in prep.

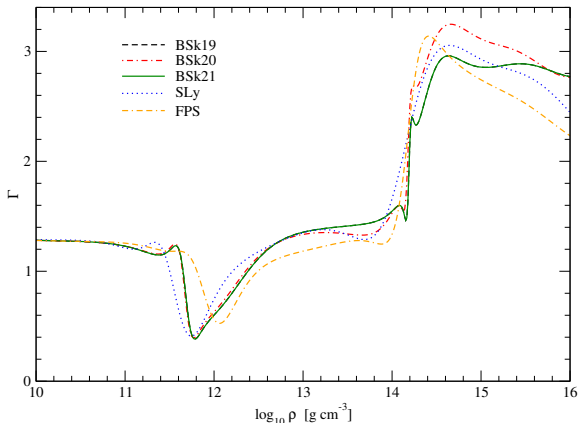
Matching of different equations of state

Ad hoc matching of different equations of state can lead to significant errors on the structure and on the dynamics of neutron stars.



Adiabatic index

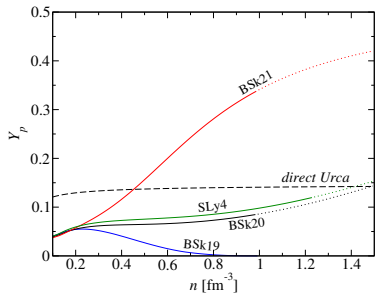
Realistic equations of state can hardly be parametrized by polytropes!



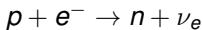
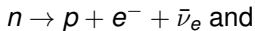
Potekhin, Fantina, Chamel, Pearson, Goriely, *A&A* 560, A48 (2013)

Neutron-star composition and direct Urca

Depending on their composition, neutron stars may cool very rapidly via the direct Urca process.



The direct Urca process

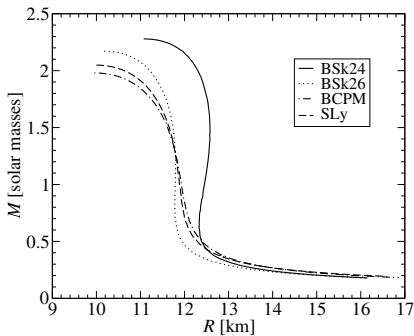
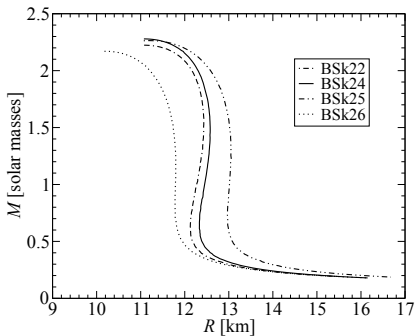


is allowed if the proton fraction Y_p exceeds a critical threshold.

The low luminosity from CTA1, SAX J1808.4–3658, 1H 1905+000 and several young supernova remnants suggest that the direct Urca has occurred. This would rule out the SLy4, BSk19 and BSk20 EoSs. *Chamel et al., Phys.Rev.C84,062802(R)(2011).*

Nuclear uncertainties in the mass-radius

Mass-radius relation of nonrotating and nonaccreting neutron stars:

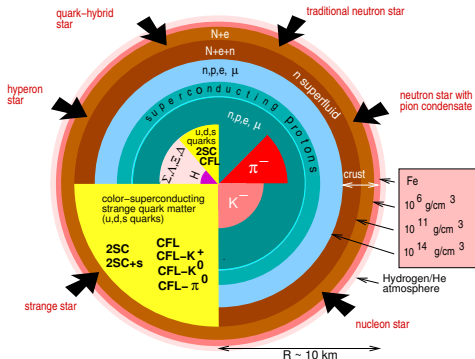


Delsate et al., Phys. Rev. D 94, 023008 (2016)

The radius of a $1.4M_{\odot}$ neutron star is predicted to lie between 11.8 and 13 km.

Exotic neutron star cores

The core of a neutron star may contain hyperons, meson condensates, or even deconfined quarks:



Microscopic approaches:

- diagrammatic
- variational
- quantum Monte Carlo

Phenomenological:

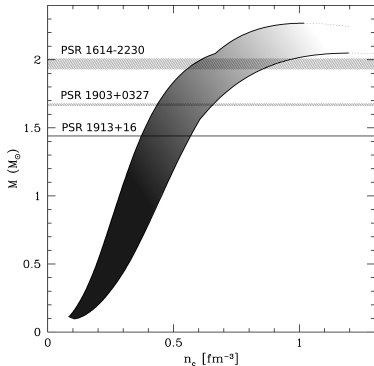
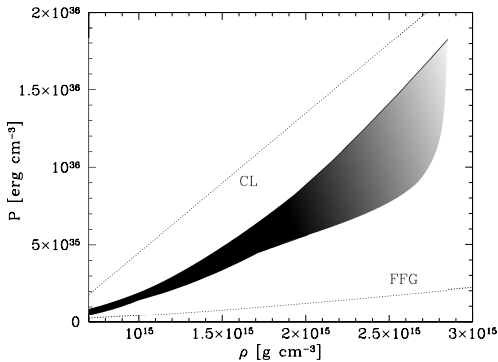
- “mean-field”

picture from F. Weber

*Alford&Sedrakian, PRL119, 161104 (2017); Oertel et al., RMP89,015007 (2017)
 Chatterjee&Vidana, EPJA52, 29 (2016); Sedrakian, Acta Phys.Pol.B3,669 (2010)*

Uncertainties in the dense-matter equation of state

Range of pressure P vs density ρ and corresponding neutron-star mass M vs central baryon density n_c , as predicted by various models consistent with the existence of massive neutron stars:



Chamel, Haensel, Zdunik, Fantina, *Int.J.Mod.Phys.E22,1330018(2013)*

Maximum neutron-star mass predictions

PSR J0348+0432 is currently the most massive neutron star with $M = 2.01 \pm 0.04 M_{\odot}$.

The core is assumed to contain nucleons (N), nucleons and hyperons (NH), nucleons and quarks (NQ).

- **Microscopic models:** (Dirac) Brueckner Hartree-Fock ((D)BHF), variational chain summation method (VCS), perturbative quantum chromodynamics (pQCD)

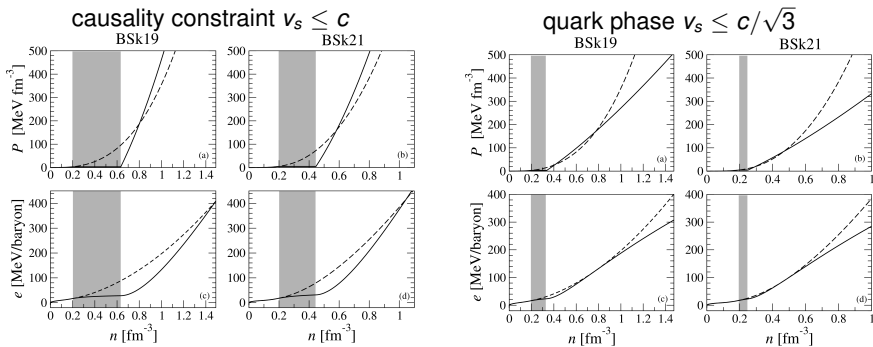
	(D)BHF (N)	BHF (NH)	VCS (N)	pQCD (NQ)
M_{\max}/M_{\odot}	2.0-2.5	1.3-1.6	2.0-2.2	2.0

- **Effective models:** Relativistic Mean Field (RMF), Nambu-Jona-Lasinio (NJL), Modified Bag Model (MBM)

	RMF (N)	RMF (NH)	RMF/NJL (NQ)	RMF/MBM (NQ)
M_{\max}/M_{\odot}	2.1-2.8	2.0-2.3	2.0-2.2	2.0-2.5

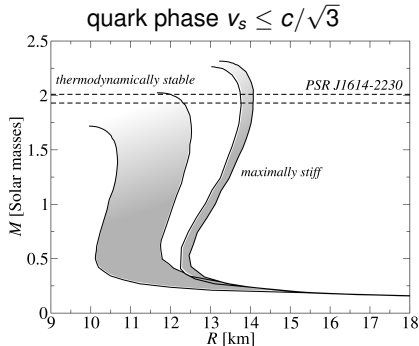
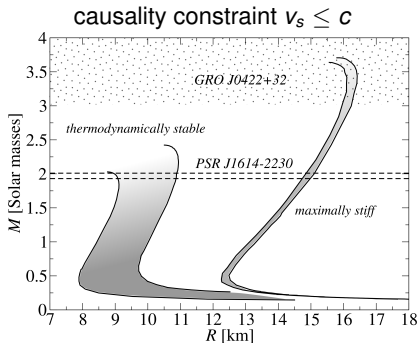
Phase transition in neutron-star cores

Given the current lack of knowledge, let us consider the occurrence of a 1st order transition to an exotic phase with the **stiffest possible thermodynamically consistent** equation of state:



Chamel, Fantina, Pearson, Goriely, A&A553, A22 (2013)

Phase transition and maximum neutron-star mass



- “Soft” nucleonic equation of state as suggested by heavy-ion collisions are not necessarily ruled out by observations.
- Neutron stars with $M > 2M_{\odot}$ would be hardly compatible with the presence of quarks in their core.

Chamel, Fantina, Pearson, Goriely, *A&A*553, A22 (2013)

Conclusions

- **Outer crust (nuclei+electrons)**: fairly well known (nuclear masses). Analytical equation of state (electron gas).
- **Inner crust (clusters+neutrons+electrons)**: composition very sensitive to magic numbers far from stability, to a less extent on the symmetry energy below saturation.

Uncertainties on the crust related to real astrophysical conditions (cooling history and crystallisation, accretion, magnetic field).

- **Liquid mantle**: nuclear pastas? Important for transport.
- **Outer core (nucleons+leptons)**: composition determined by symmetry energy above saturation.
- **Inner core (?)**: highly speculative but constraints on the equation of state imposed by the existence of massive stars.

- Thermodynamically inconsistencies can lead to significant errors on neutron star structure and dynamics (ad hoc matching)
- Unified equations of state treating all regions can hardly be parametrised by polytropes.